Polymer Chemistry

ROYAL SOCIETY OF CHEMISTRY

PAPER

View Article Online
View Journal | View Issue

Cite this: *Polym. Chem.*, 2020, **11**, 6910

Time-dependent covalent network formation in extrudable hydrogels†

Dylan Karis and Alshakim Nelson *

The fabrication of hydrogel materials has gained increased attention for a broad range of biomedical and biotechnological applications. However, one longstanding challenge in the field is to develop hydrogels that can be easily processed into the desired form factor, while achieving the necessary final physical and biochemical properties. Herein, we report a shear-thinning hydrogel ink that can be photo-cured to create a stretchable, suturable hydrogel whose polymer network is formed *via* the combination of thiol-Michael addition and radical polymerization. A shear-thinning hydrogel based on bis-methacrylated Pluronic® F-127 was modified with varying equivalents of 2,2′-(ethylenedioxy)diethanethiol (EDT) as an additive. We observed that aging the hydrogel over time prior to extrusion allowed the relatively slow thiol-Michael addition to occur (between thiol and methacrylate) prior to UV initiated photo-polymerization of the methacrylates. The viscoelastic properties of these hydrogels could be tuned based on the amount of EDT added, and the aging time of the hydrogel formulation. The changes to the physical properties of the hydrogels were attributed to the increased chain length between network junctions that resulted from the thiol-Michael addition reactions. The optimized hydrogel composition was then extruded from a coaxial nozzle to produce hydrogel tubes that, after curing, were resistant to tearing and were suturable. These extrudable synthetic hydrogels with tunable viscoelastic properties are promising for tissue engineering applications and as surgical training models for human vasculature.

Received 8th August 2020,
Accepted 7th September 2020

DOI: 10.1039/d0py01129k

rsc.li/polymers

Introduction

Hydrogels are an important class of material due to their widespread use in biomedical applications such as tissue engineering,[1–13] surgical training models,[14,15] and implantable devices.[14,16–19] Synthetic polymer hydrogels are advantageous over naturally derived hydrogels (such as calcium alginate and gelatin) because they afford materials that can be more specifically tailored to mimic biological materials like human tissue.[20–22] However, one longstanding challenge in the field is to develop hydrogels that can be easily processed into the desired form factor, while achieving the necessary final physical and biochemical properties. Shear-thinning hydrogels[23,24] have shear-dependent viscoelastic behaviors that can facilitate the processing of these materials, and are particularly well-suited as injectable hydrogels for subdermal drug delivery[25–27] and for direct ink write 3D printing.[28–30] These hydrogels can be mechanically or pneumatically pressurized to flow from a syringe, and can quickly recover its gel state *via* the reformation of reversible covalent or noncovalent bonds upon exiting the nozzle.[31,32] Strategies for designing shear-thinning hydrogels have included incorporation of cyclodextrin to enable host–guest supramolecular interactions,[28] protein directed assembly,[33] and control of block copolymer architectures.[34–36]

Poly(ethylene oxide)-*b*-poly(propylene oxide)-*b*-poly(ethylene oxide) is a triblock copolymer that self-assembles into micelles in water to afford shear-thinning hydrogels. Our group,[29,37–41] and others,[42,43] have used a commercially available form of this polymer known as F127, and the cross-linkable F127-bisurethane methacrylate (F127-BUM) derivative, to afford extrudable hydrogel inks for creating 3D constructs. In a recent example, we extruded hydrogel tubes toward modeling vascular endothelium using customized coaxial nozzles.[38] The nozzles were modeled *via* computer-aided design and then 3D printed on a commercially available SLA printer to generate coaxial nozzles with different orifice geometries and dimensions. While the lumen of these tubular hydrogel constructs could be endothelialized with human umbilical vein endothelial cells, the hydrogels were still limited by their brittleness, particularly to needle puncture during suture. Thus,

Department of Chemistry, University of Washington, Seattle, Washington 98105, USA. E-mail: alshakim@uw.edu

†Electronic supplementary information (ESI) available: ^{1}H NMR spectra of synthesized polymer, additional rheological tests, and videos of relevant hydrogels. See DOI: 10.1039/d0py01129k

chemical strategies that provide the processability of hydrogels *via* shear-thinning behavior, but with improved mechanical properties after curing the hydrogels are desirable for engineering *in vitro* models that resemble tubular biological structures (such as blood vessels, airways, and the intestines).

Thiol-Michael "click" chemistry presents an important class of reactions for macromolecular systems[44–46] that has been utilized in bioconjugation reactions,[47–49] the formation of graft polymer architectures,[50,51] and network formation in polymer hydrogels.[3,52–56] The thiol-Michael addition takes place between a free thiol and α,β-unsaturated ester and may be catalyzed by base, or phosphorus and nitrogen centered nucleophiles.[57] As demonstrated in a computational study by Northrop and Coffey, methacrylates are generally less reactive than acrylates, ally ethers, and maleimides in thiol-Michael reactions.[58] Bowman and co-workers experimentally verified this difference in reactivity by using a photobase and show slow addition of thiols onto butyl methacrylate.[59] Additionally, thiols and alkenes can undergo photoradical thiol-Michael reactions. Bunel and co-workers showed that under photoradical conditions, methacrylate homopolymerization was favored over photoradical thiol-Michael addition.[60]

Recently, Long and co-workers showed that the combination of free-radical polymerization with thiol-Michael "click" chemistry could be utilized to afford poly(dimethylsiloxane)-based (PDMS-based) silicones. The chain-ends of PDMS were functionalized with acrylamides or thiols to afford resins that varied in the ratio of thiol to acrylamide. The polymerized network showed a tunable stretchability and Young's modulus that was dependent upon the extent of thiol-Michael chain-extension between chain-end acrylamide and thiols, *versus* the free-radical polymerization of the chain-end acrylamides.[61] The Smaldone group has also demonstrated base-catalyzed thiol-Michael addition of a three-arm thiol onto acrylate-functionalized F127. In this work, the concentration of base determined the cross-link density of the final printed construct.[62] Additionally, Anseth and co-workers demonstrated the importance of aging in gels formulated with thiols. Their group used a four-arm thiol and diacrylated PEG to show a time-dependent thiol-Michael addition, which forms the preliminary polymer network before a subsequent UV cure further cross-links the material.[63]

Herein, we report a shear-thinning hydrogel ink that can be photo-cured to create a stretchable, suturable hydrogel whose polymer network is formed *via* the combination of thiol-Michael addition and radical polymerization. The introduction of a dithiol additive into the F127-BUM hydrogel was employed to introduce two different covalent bond-forming reactions: the radical polymerization of the methacrylate chain-ends cross-links the polymer network, while the thiol-Michael coupling reaction of the F127 polymer chains with a dithiol additive could effectively increase the molecular weight of the polymer chains between cross-linking sites (Fig. 1). As a result, the mechanical properties of the hydrogels were dependent upon the contribution of the thiol-Michael addition *versus* the radical polymerization to the formation of the final network.

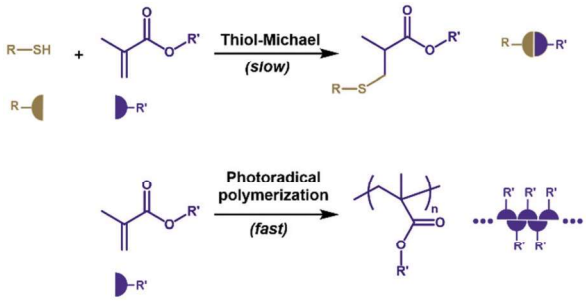

Fig. 1 The scope of reactions available between thiols and methacrylates. A slow thiol-Michael reaction takes place spontaneously while introduction of lithium phenyl-2,4,6-trimethylbenzoylphosphinate (LAP) photoinitiator and 365 nm light enables fast photoradical mediated polymerization.

Although the thiol-Michael addition between thiols and methacrylates is slow, the hydrogel ink can be aged over time to allow the reaction to occur prior to the UV-initiated radical polymerization of the methacrylate end-groups. The hydrogel inks were extruded using a coaxial nozzle to create tubular constructs that were UV-cured to afford suturable hydrogels, which could have future use as models for vascular tissue.

Experimental

Materials and instrumentation

All chemicals and solvents, unless otherwise stated, were purchased from Sigma-Aldrich or Fisher Scientific and used without further purification unless noted otherwise. Pluronic® F127 was dried under reduced pressure overnight prior to functionalization. Dry dichloromethane was obtained by purification over alumina columns on a Pure Process Technology purification system. ^{1}H NMR spectra were obtained on a Bruker Avance 300 or 500 MHz spectrometer.

Synthesis of pluronic® F127-bis-urethane methacrylate (F127-BUM)

The synthesis of F127-bis-urethane methacrylate (F127-BUM) was performed as previously described.[38] Briefly, F127 (60 g, 4.8 mmol) was dried under vacuum, then anhydrous dichloromethane (550 ml) was charged to the flask. The mixture was stirred until complete dissolution of the F127 was observed. Dibutyltin dilaurate (12 drops) was then added, followed by dropwise addition of 2-isocyanatoethyl methacrylate (3.5 ml, 24.8 mmol) in anhydrous dichloromethane (50 ml). The reaction was allowed to proceed for 2 d before quenching with MeOH. The F127-BUM was precipitated in ether, allowed to settle, and decanted. The F127-BUM precipitate was finally washed in ether twice, prior to being dried under vacuum. ^{1}H NMR (500 MHz, $CDCl_3$): δ 3.38–3.77 (m, 4H, PEG backbone, PPO backbone), 1.12 (d, 3H, PPO methyl).

Preparation of F127-BUM hydrogels

F127-BUM (3 g, 0.24 mmol) was added to a scintillation vial, then deionized water (7 mL) was added. The vial was then vortex mixed and placed in an ice box until fully dissolved. To this vial, lithium phenyl-2,4,6-trimethylbenzoylphosphinate (LAP, 10 mg, 0.03 mmol) and 2,2′-(ethylenedioxy)diethanethiol (EDT, 58.6 μL, 0.36 mmol) were added and stirred ~5 °C until fully dissolved. Samples were stored in a 5 °C refrigerator and only removed at 0, 1, 3, 7, and 14 d time points to be cast into molds or loaded onto the rheometer.

Rheological experiments

Viscous flow experiments were performed on a TA Instruments Discovery HR-2 equipped with a 40 mm cone and plate geometry. Samples, which were equilibrated in an ice bath for at least 10 min, were carefully loaded onto a Peltier plate at 5 °C and trimmed. A preshear experiment was conducted to ensure that bubbles were eliminated from the sample cell. The sample was equilibrated at 21 °C for 8 min. The experiments were conducted in a logarithmic sweep from 0.01 to 100 s^{-1} with 5 points per decade. Data was collected using steady state sensing with a 30 s sample period, 5% tolerance, and 3 consecutive measurements. Photorheological experiments were performed with an 8 mm parallel plate geometry and loaded onto a UV curing stage. A preshear experiment was conducted to ensure that bubbles were eliminated from the sample cell. The sample was equilibrated at room temperature for 8 min. The photorheological experiments were conducted using constant 1% strain and a frequency of 1 Hz which lies in the linear viscoelastic regime. A 120 s dwell time elapsed before the UV lamp (365 nm LED with an irradiation intensity of 5 mW cm^{-2}) was turned on for 7 min.

Tensile measurements

An Instron 5585H 250 kN electro-mechanical test frame with a 50 N load cell was used to evaluate the tensile properties of the cross-linked hydrogels. The ASTM D638 type V specimen specifications were used to prepare dogbone samples by casting in approximately 2 g of 30 wt% gel into a Teflon dogbone mold. The gel was then exposed to 365 nm light for 10 min. The chemically cross-linked structure was then removed from the mold and placed into a Falcon tube with a hydrated KimWipe to maintain humidity before testing. The sample was then placed on pneumatic self-aligning grips fixed on the load frame, and the sample was subjected to increasing strain at a constant rate of 10 mm min^{-1} until mechanical failure of the sample. Axial strain was measured with a video extensometer accessory. Young's modulus was calculated from the slope of the linear region between 0 to 10% strain.

Compressive measurements

An Instron 5585H 250 kN electro-mechanical test frame with a 1 kN load cell was used to evaluate the compressive properties of the cross-linked hydrogel. Cylindrical compression samples (10 mm diameter × 5 mm height) were cast into PDMS molds and then exposed to 365 nm light for 10 min. The chemically cross-linked structure was then removed from the mold and placed into a Falcon tube with a hydrated tissue to maintain humidity before testing. All tests were conducted at room temperature (21 °C) using a crosshead rate of 1.3 mm min^{-1} until 80% strain. Compressive modulus was calculated from the slope of the linear region between 0 to 10% strain.

Extrusion through coaxial nozzle

All tubes were extruded through custom printed coaxial nozzles[38] with a Form 2 SLA 3D printer. Gels chilled on ice were loaded into syringes (Nordson EFD), and once the gels reached room temperature, the extrusion set-up was assembled. Syringe barrel adapters (Nordson EFD) were then attached to each syringe. Pressure to drive the syringe pistons (10–12 psi) was supplied by an in-house N_2 line. To adjust pressures prior to extrusion, the tubing of each syringe barrel adapter was clamped using a pinch-clamp, and the regulators were set to the desired pressures. To begin extrusion, the tubing of each adapter was unclamped, and after waiting a moment for the coaxial extrusion rate to stabilize, a 4 in × 6 in glass sheet was manually translated under the nozzle to catch the coaxial gel filament. The shell of the coaxial filament was then photo cross-linked for 10 min under a UV lamp (365 nm, 3.3 mW cm^{-2}).

Degree of swelling and gel fraction experiments

Cylindrical samples (10 mm diameter × 5 mm height) were cast into PDMS molds and then exposed to 365 nm light for 10 min. The resulting cross-linked gel was extracted and wiped down to remove residual uncross-linked polymer on the surface and weighed. The disks were then dried in a vacuum oven for 1 d and weighed to obtain the initial dry mass. Equilibrium swelling was achieved by soaking the disks in DI water over 3 d and weighed to obtain the degree of swelling. The swollen gels were then dried in a vacuum oven for 2 d and weighed to obtain a second dry mass which was used to calculate the gel fraction (G_f).

Suturability tests

Hydrogel tubes extruded using a coaxial nozzle were first cut using a razor blade. To the middle of the tube, a plastic insert was placed to provide structural support. A 4/0 nylon suture was used to rejoin the material. The simple interrupted suture method was used to demonstrate suturability. The final sutured tube was washed in DI water and the plastic insert was removed. The hydrogels were robust and could easily be handled after suturing. However, dehydration or excessive swelling can change the mechanical properties of the hydrogel.

Results and discussion

F127-BUM affords shear-thinning hydrogels at concentrations above ~20 w/w%, even in the presence of water-soluble addi-

tives.[29] In this investigation, 2,2′-(ethylenedioxy) diethanethiol (EDT) was introduced as an additive to 30 w/w% F127-BUM hydrogel formulations (with 0.1 wt% LAP as photo-initiator) (Fig. 2) at 0, 0.5, 1.0, 1.5, or 2.0 molar equivalents relative to the polymer. Rheological characterization of these hydrogels confirmed the shear-thinning behavior of all the hydrogels (Fig. S7–10†). Fig. 1 shows the reactions by which covalent networks can be formed. Thiols can spontaneously react with methacrylates at a slow rate under ambient conditions and neutral pH (in the absence of UV light). This reaction results in a chain-extension that couples F127-BUM polymer chains to form longer bridging chains between points of cross-linking in the network. Photoinitiated radical polymerization of the methacrylate end-groups can also occur rapidly and introduces crosslinking sites into the network. As shown in Fig. 2, the final polymer network is comprised of both physical cross-links (the assembled poly(propylene oxide) blocks of the self-assembled micelle core) and chemical cross-links (the polymerized methacrylate chain-ends) that are separated by the bridging polymer chains.

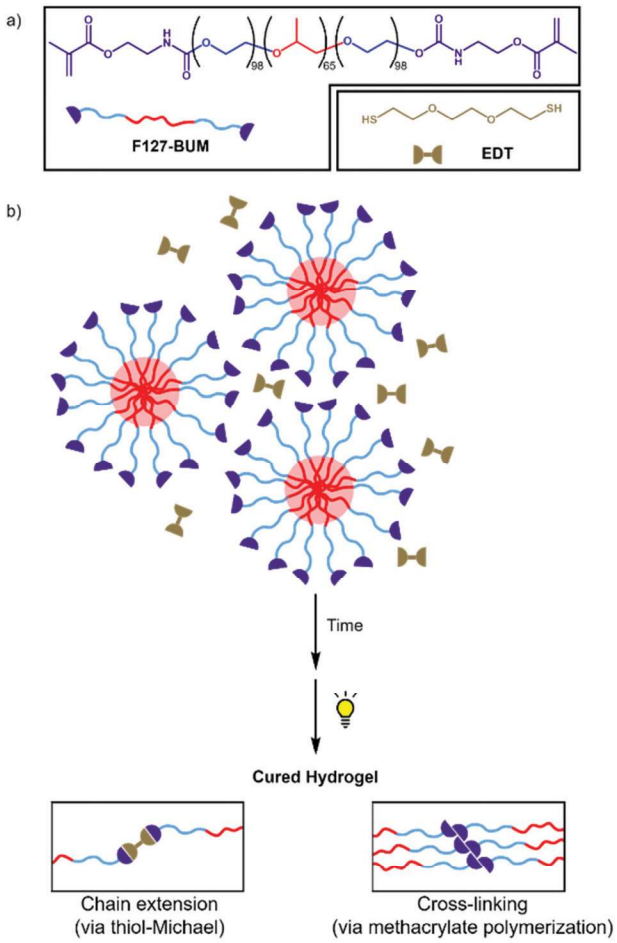

Fig. 2 (a) Materials used in this work. F127 is functionalized with urethane methacrylate end-groups (F127-BUM). At temperatures above the gelation temperature (T_{gel}) and in concentrations greater than 20 wt%, F127-BUM forms core–shell micelles that affords a hydrogel network. 2,2′-(ethylenedioxy)diethanethiol (EDT) was chosen because of its water solubility and commercial availability. (b) An F127-BUM hydrogel formulated with EDT slowly undergoes thiol-Michael chain-extension. A UV cure after a set period of ageing affords tunability in the extent of cross-linking by radical polymerization.

F127-BUM hydrogels that are chemically cross-linked in the absence of EDT exhibit elasticity, and brittle fracture upon failure. Inspired by recent publications on 3D printed elastomers,[61,64] we hypothesized that increasing the length of the bridging F127-BUM chains *via* thiol-Michael addition could lead to hydrogel networks tunable stiffness and stretchability. As a method of characterizing hydrogel networks, the affine network theory of unentangled rubber elasticity[65] is a useful tool to help probe the effects of cross-link junctions. This model assumes that the cross-link points between each strand is representative of the entire network and may estimate the molecular weight between cross-link junctions through uniaxial deformation written in terms of the shear modulus. F127 is known to create hydrogel networks by the aggregation of micelles packing into a face-centered cubic (fcc) lattice at concentrations above 20 wt% in aqueous media and above its gelation temperature (T_{gel}).[66] This model does not take into account defects such as loops or dangling ends and may not be representative of a highly entangled micellar network such as F127. Nonetheless, many groups have shown that this is an appropriate model for this type of investigation.[61,67–69] Eqn (1) allows us to approximate the molecular weight between cross-links (M_c) by using rheometry to determine the average plateau storage modulus (G^0_N).

$$M_c = \frac{dRT}{G^0_N} \quad (1)$$

where d is density, T is temperature, and R is the universal gas constant.

The shear moduli of all hydrogel formulations were determined using a photo-rheometer in which the samples were exposed to 365 nm light and the viscoelastic properties monitored over that time. Given the slow kinetics of thiol-Michael addition in reactions that involve methacrylates in the absence of any catalyst, each hydrogel formulation was characterized over the course of 14 days.

The thiol-Michael reaction (slow rate of reaction) and photo-initiated radical polymerization (fast rate of reaction) occurred during two discrete steps. Upon addition of EDT to each hydrogel formulation the thiols can undergo a spontaneous thiol-Michael addition to extend the polymer chains. After a predetermined period of time (on the order of days) the photopolymerization of the methacrylates was initiated upon UV exposure during the photo-rheology experiment. Representative examples of the photo-rheological experiments from days 0 and 7 are shown in Fig. 3a and b. Upon UV irradiation (365 nm, 5 mW cm^{-2}) the storage modulus rapidly increased within 2 min to a plateau storage modulus (G^0_N). Initially (at day 0), the (G^0_N) for the hydrogels were similar, independent of the quantity of EDT that was added. In this case, the thiol-Michael reactions were too slow to enable

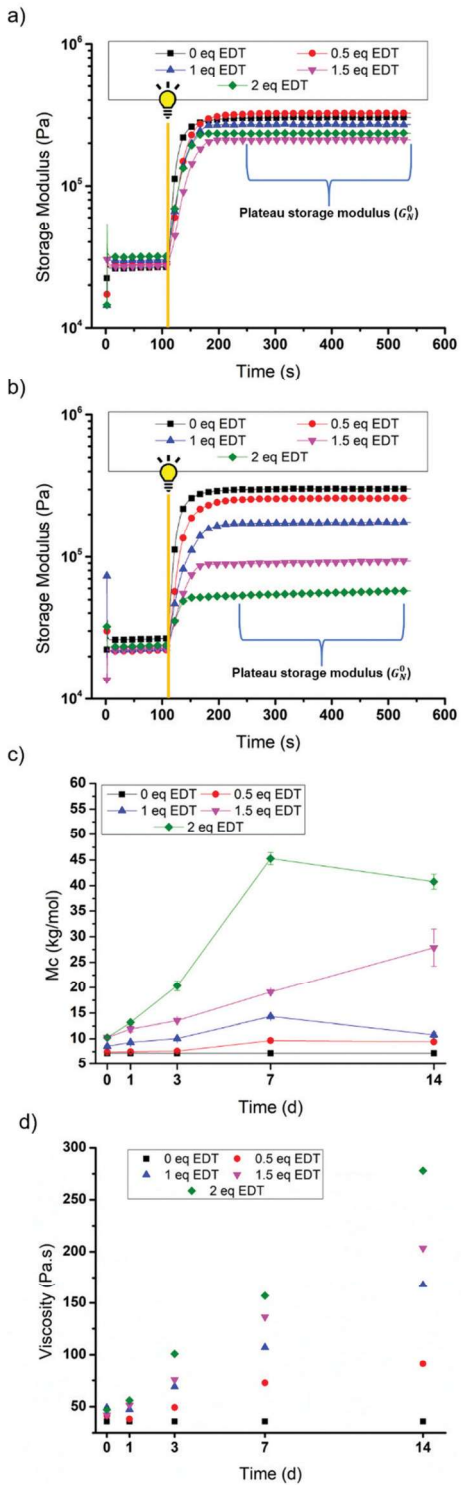

Fig. 3 Photorheological characterization of 30 wt% F127-BUM hydrogel with varying equivalents of EDT after (a) 0 and and (b) 7 days of equilibration. At 120 s, the UV light was turned on and left on for the remainder of the experiment. The plateau storage modulus was taken as the average storage modulus in the region between 250 and 550 s. (c) Molecular weight between cross-links (M_c) as calculated from eqn (1). A linear increase was shown for 1 to 2 equivalents EDT in the first 7 days. (d) Viscosity measurements taken at 10 s^{-1} at 21 °C. Apart from unmodified F127-BUM, each formulation shows a linear increase in viscosity over time, which suggests an increase in molecular weight prior to UV cure.

sufficient incorporation of EDT into the polymer network. However, as we increased the time (day 3 and beyond) for the thiol-Michael reaction to occur prior to photo-initiated polymerization, larger differences were observed based on the molar equivalents of EDT (Fig. 3a and b). For example, in the case of the samples that were incubated for 7 days prior to photo-initiated polymerization, as the molar equivalents of EDT in the hydrogel formulation was increased, the G_N^0 for that hydrogel decreased. Thus, while the F127-BUM hydrogel had a G_N^0 of 347 kPa, the hydrogel formulation with highest amount of EDT (2 molar equivalents) in this study exhibited a decreased stiffness (55 kPa). We attribute this trend to the increase in length of the polymer chains (the total length of bridging chains increase as F127 polymer chains are coupled together *via* thiol-Michael addition reactions) relative to free-radical polymerization of the methacrylates as the thiol : alkene ratio increased.

The relative stiffness between the different formulations can be used to determine the molecular weight between cross-links (M_c) by using a calculation derived from the affine theory of rubber elasticity (eqn (1)). The number average molecular weight for F127-BUM is 12.5 kg mol^{-1}, which corresponded well to the values obtained using Kuhn's model for day 0 and day 1 (Fig. 3c). During these earlier time periods, there was not a significant change to the molecular weight (8–12 kg mol^{-1}) independent of the amount of EDT that was added. The slow kinetics of the thiol-Michael reaction meant that there was negligible chain extension. However, M_c increased over time (see days 3, 7, and 14 in Fig. S3–5†) when 1.5 equivalents or 2.0 equivalents of EDT was included in the formulation. Thus, there was chain extension *via* bridging thiol-Michael addition over time.

Further support for thiol-Michael addition prior to UV curing was provided by rheometrical evaluation of the changes in the viscosity of the hydrogels (Fig. 3d). During the early time periods, there was little variation in the viscosity of the hydrogel. However, after 3 days, the viscosity began to deviate from 49 to 100 Pa s^{-1} and continued to increase linearly over 14 days to 91 and 278 Pa s^{-1} for 0.5 and 2 equivalents, respectively. These results suggest that chain-extension from slow thiol-Michael addition led to an increase in molecular weight in a time-dependent manner prior to polymerization by UV light.

Given the possibility of dead chain-ends influencing the M_c value, measurements on the degree of swelling and gel fraction were performed to offer insight into the cross-link density and the ability of non-polymerized units to leach out of the network. As shown in Fig. 4a, the hydrogels with 1 or fewer equivalents of EDT maintain around the same degree of swelling, whereas 1.5 and 2 equivalents aged for 7 days increase to 10 and 26 times their dry mass, respectively. These results are supported by a gel fraction (G_f) experiment (Fig. 4b) where the swollen gels were then subsequently dried *in vacuo* and weighed. G_f was calculated by taking the dried mass after equilibrium swelling over the initial dried mass to determine the amount of polymer covalently incorporated into the network.

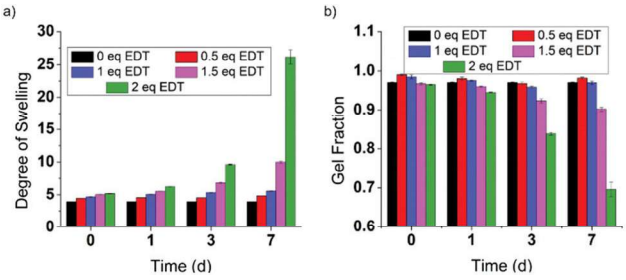

Fig. 4 Swelling experiments performed on 30 wt% F127-BUM with varying equivalents of EDT. (a) Degree of swelling shows a drastic increase when using 2 equivalents of EDT. (b) Gel fraction experiment showing that 30% of the polymer mass is lost when 2 equivalents of EDT are added to the hydrogel formulation.

The source of the increased degree of swelling could come from the net loss of cross-linking polymer chains from the network (10 and 30% polymer mass for 1.5 and 2 equivalents of EDT, respectively). To determine the effect of dead chain-ends on the M_c, we compared 3 equivalents of mercaptoethanol (which has one reactive thiol) to 1.5 equivalents of EDT (which has two reactive thiols) to achieve the same thiol : alkene ratio. The M_c value was 42 kg mol^{-1} after ageing the mercaptoethanol-containing hydrogel for 3 days compared to 19 kg mol^{-1} for the EDT containing sample (Fig. S6†). Additionally, the mercaptoethanol containing gel completely dissolved after 3 days of ageing. Thus, EDT may contribute to the presence of dead chain ends, but was largely incorporated into the polymer network and contributed to the increased degree of swelling.

Fig. 5a shows a representative set of tensile measurements from 0 to 1.5 equivalents of EDT for hydrogel formulations that were aged for 3 days. The data for the hydrogel comprising 2 equivalents of EDT is not shown due to elongation beyond the video extensometer's active window. We observed that as the amount of thiol was increased, the Young's modulus (Y) decreased and the elongation at break increased, which suggests a more stretchable hydrogel. Compression experiments on the same set of gels showed similar trends (Fig. 5b), as summarized in Table 1. At higher equivalents of EDT, there was a greater degree of chain-extension *via* thiol-Michael addition which reduced the stiffness of a resulting hydrogel.

In an extrusion-based setup, shear-thinning gel viscosity (Fig. S7–10†) is an important parameter to determine how well

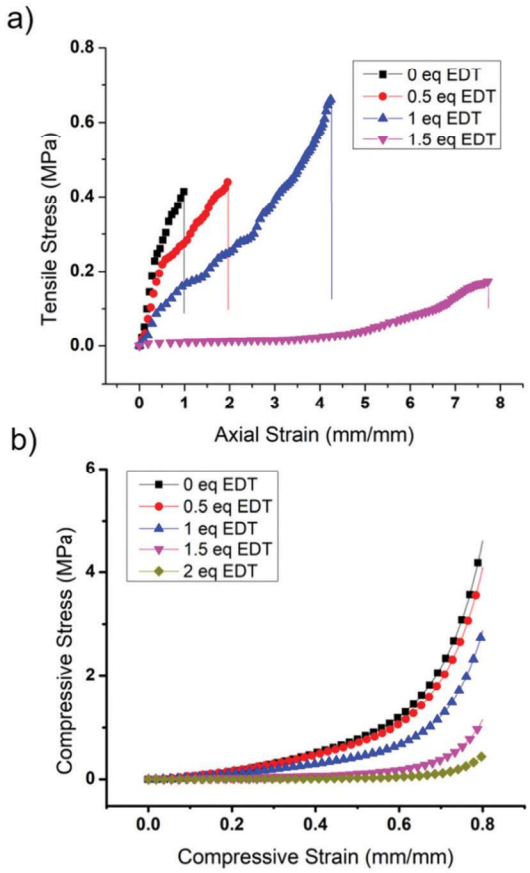

Fig. 5 Tensile and compression measurements taken on the third day after adding EDT to a 30 wt% F127-BUM hydrogel. (a) Stress–strain tensile curve showing increased stretchability with higher EDT equivalents. 2 eq. EDT omitted because the dogbone extended beyond the video extensometer viewing window. (b) Stress–strain compression curve showing a reduction in maximum stress at 80% extension. Tabulated Young's and compressive moduli can be found in Table 1.

the material will flow out of a nozzle. In general, we observed that hydrogel formulations with viscosities greater than 100 Pa s^{-1} (Fig. 3d) did not readily extrude from a pneumatically controlled syringe at 20 psi. Therefore, aging of the hydrogels beyond 7 days and with ≥1.5 equivalents resulted in gels that could not be extruded. Additionally, stiff hydrogels were not capable of withstanding a needle puncture without tearing. As evidenced by tensile measurements (Fig. 5a), hydro-

Table 1 Summary of tensile and compression experiments for 30 wt% F127-BUM with varying equivalents of EDT after 3 days of equilibration

Dithiol eq	Y [a,c] (MPa)	E [a,c] (MPa)	Max elongation at break (mm mm^{-1})	Max compressive stress [b,c] (MPa)
0	1.0 ± 0.1	1.1 ± 0.1	0.55 ± 0.08	5 ± 1
0.5	0.78 ± 0.07	0.98 ± 0.03	2.0 ± 0.2	4.6 ± 0.9
1	0.54 ± 0.04	0.654 ± 0.006	3.2 ± 0.5	2.8 ± 0.2
1.5	0.25 ± 0.03	0.26 ± 0.03	8 ± 1	1.1 ± 0.1
2	0.04 ± 0.01	0.039 ± 0.004	24.9 ± 0.9	0.44 ± 0.06

[a] Calculated as the linear region between 0 and 10% extension. [b] Reported at 80% extension. [c] Error given as standard deviation over 3 replicate experiments.

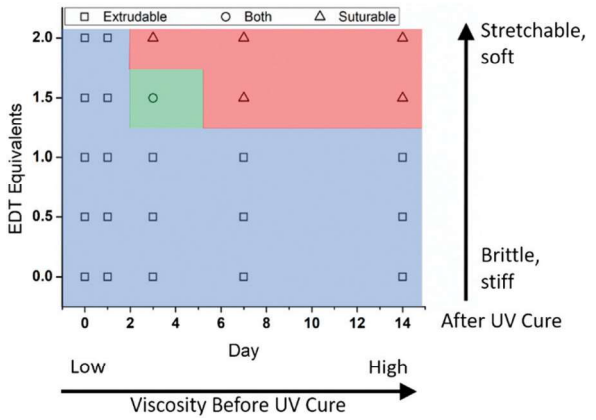

Fig. 6 Summary of extrudability and Suturability in EDT containing F127-BUM hydrogels. Ageing the hydrogel increases the viscosity while increasing the EDT equivalents results in a suturable gel. The optimum conditions are 1.5 equivalents EDT aged for 3 d.

gels with 1 or fewer EDT equivalents resulted in stiff and brittle gels (see ESI Videos†), while hydrogels with 2 equivalents underwent plastic deformation. We observed that 1.5 equivalents of EDT in the hydrogel aged for 3 days resulted in an elastic hydrogel that could resist tearing or fracturing when punctured with a needle (Fig. 6).

Finally, we demonstrated the extrusion of a hydrogel tube using an optimized hydrogel formulation that could be cut, and then sutured. The hydrogel formulation comprising 30 w/w% F127-BUM and 1.5 equivalents of EDT was aged for 3 days prior to extrusion through a custom nozzle[38] that affords tubular hydrogel constructs (Fig. 7). After irradiation with UV light, the samples were cross-linked *via* radical polymerization to afford stretchable hydrogel tubes. The extruded hydrogel tube was then cut with a razor blade and a plastic support piece was installed, before a nylon 4/0 monofilament suturing needle was passed through the gel on both ends and set with a simple suture. Finally, the plastic support was removed, and the hydrogel was washed to show the suture remaining in place. The resulting stitched hydrogel was robust and could be manipulated by hand without tearing the suture.

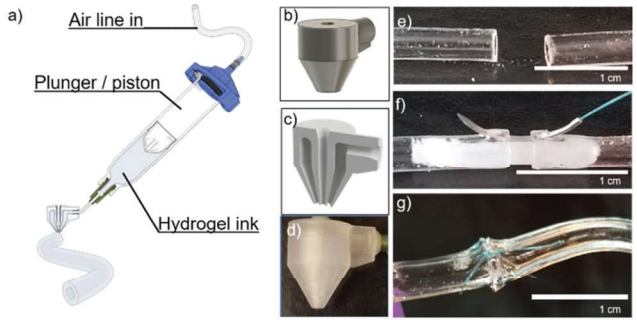

Fig. 7 Fabrication and suturing of 30 wt% F127-BUM hydrogel with 1.5 equivalents EDT and equilibrated for 3 days. (a) Cartoon of coaxial nozzle extrusion setup showing cross-section of nozzle and final printed hollow hydrogel tube. (b) STL rending of nozzle, (c) cross section, and (d) printed nozzle using Form 2 clear resin. (e) After extrusion, the tube is cut down the middle. (f) A plastic insert is placed as a support for the 4/0 nylon monofilament needle to join the two tubes. (g) A simple interrupted suture is placed, the plastic insert is removed, and the hydrogel is washed.

Conclusion

A stretchable, suturable hydrogel was fabricated utilizing a shear-thinning hydrogel that could undergo a combination of thiol-Michael chain-extension and free-radical polymerization. The ratio of dithiol additive to methacrylate was altered to tune the viscoelastic properties of the hydrogel. Through use of the affine network theory of rubber elasticity, the molecular weight between cross-links was calculated and provides support for explaining the difference in mechanical properties of the hydrogels. The proposed mechanism of network formation occurs *via* a slow thiol-Michael addition during a period of hydrogel aging, followed by free-radical polymerization initiated by UV light. In our study, we observed that 3 days of equilibration with a 1.5 : 1 thiol : methacrylate ratio was optimal to achieve good stretchability and resistance to tear during suture. This hydrogel was extruded through a custom 3D printed nozzle to afford robust, suturable hydrogel tubes. These materials represent a promising step toward synthetic vasculature for surgical training and implantable devices.

Conflicts of interest

The authors have no conflicts to declare.

Acknowledgements

We acknowledge Siyami (Cem) Millik for guidance on the extrusion of coaxial tubes. We gratefully acknowledge support from the National Science Foundation (1752972) for this work.

Notes and references

1 D. Joung, N. S. Lavoie, S. Z. Guo, S. H. Park, A. M. Parr and M. C. McAlpine, *Adv. Funct. Mater.*, 2020, **30**, 1906237.
2 R. D. Pedde, B. Mirani, A. Navaei, T. Styan, S. Wong, M. Mehrali, A. Thakur, N. K. Mohtaram, A. Bayati, A. Dolatshahi-Pirouz, M. Nikkhah, S. M. Willerth and M. Akbari, *Adv. Mater.*, 2017, **29**, 1606061.
3 Z. Jiang, R. Shaha, R. McBride, K. Jiang, M. Tang, B. Xu, A. K. Goroncy, C. Frick and J. Oakey, *Biofabrication*, 2020, **12**, 035006.
4 H. W. Kang, S. J. Lee, I. K. Ko, C. Kengla, J. J. Yoo and A. Atala, *Nat. Biotechnol.*, 2016, **34**, 312–319.
5 A. Lee, A. R. Hudson, D. J. Shiwarski, J. W. Tashman, T. J. Hinton, S. Yerneni, J. M. Bliley, P. G. Campbell and A. W. Feinberg, *Science*, 2019, **365**, 482–487.

6 C. Cleversey, M. Robinson and S. M. Willerth, *Micromachines*, 2019, **10**, 501.
7 S. Ahadian, R. B. Sadeghian, S. Salehi, S. Ostrovidov, H. Bae, M. Ramalingam and A. Khademhosseini, *Bioconjugate Chem.*, 2015, **26**, 1984–2001.
8 E. Jabbari, J. Leijten, Q. Xu and A. Khademhosseini, *Mater. Today*, 2016, **19**, 190–196.
9 X. Guan, M. Avci-Adali, E. Alarçin, H. Cheng, S. S. Kashaf, Y. Li, A. Chawla, H. L. Jang and A. Khademhosseini, *Biotechnol. J.*, 2017, **12**, 1600394.
10 P. S. Gungor-Ozkerim, I. Inci, Y. S. Zhang, A. Khademhosseini and M. R. Dokmeci, *Biomater. Sci.*, 2018, **6**, 915–946.
11 J. M. Knipe and N. A. Peppas, *Regener. Biomater.*, 2014, **1**, 57–65.
12 M. I. Neves, M. E. Wechsler, M. E. Gomes, R. L. Reis, P. L. Granja and N. A. Peppas, *Tissue Eng., Part B*, 2017, **23**, 27–43.
13 K. Elkhoury, C. S. Russell, L. Sanchez-Gonzalez, A. Mostafavi, T. J. Williams, C. Kahn, N. A. Peppas, E. Arab-Tehrany and A. Tamayol, *Adv. Healthcare Mater.*, 2019, **8**, 1900506.
14 K. Qiu, G. Haghiashtiani and M. C. McAlpine, *Annu. Rev. Anal. Chem.*, 2018, **11**, 287–306.
15 H. Maruyama, Y. Yokota, K. Hosono and F. Arai, *Sensors*, 2019, **19**, 1102.
16 W. Hu, Z. Zhang, L. Zhu, Y. Wen, T. Zhang, P. Ren, F. Wang and Z. Ji, *ACS Biomater. Sci. Eng.*, 2020, **6**, 1735–1743.
17 T. Sultana, H. Van Hai, C. Abueva, H. J. Kang, S. Y. Lee and B. T. Lee, *Mater. Sci. Eng., C*, 2019, **102**, 12–21.
18 Y. Wang, W. Zhu, K. Xiao, Z. Li, Q. Ma, W. Li, S. Shen and X. Weng, *Biochem. Biophys. Res. Commun.*, 2019, **508**, 25–30.
19 X. Chen, M. Wang, X. Yang, Y. Wang, L. Yu, J. Sun and J. Ding, *Theranostics*, 2019, **9**, 6080–6098.
20 L. A. Sawicki, E. M. Ovadia, L. Pradhan, J. E. Cowart, K. E. Ross, C. H. Wu and A. M. Kloxin, *APL Bioeng.*, 2019, **3**, 016101.
21 M. W. Tibbitt and K. S. Anseth, *Biotechnol. Bioeng.*, 2009, **103**, 655–663.
22 G. Papavasiliou, S. Sokic and M. Turturro, in *Biotechnology - Molecular Studies and Novel Applications for Improved Quality of Human Life*, InTech, 2012.
23 M. Guvendiren, H. D. Lu and J. A. Burdick, *Soft Matter*, 2012, **8**, 260–272.
24 E. Jalalvandi and A. Shavandi, *J. Mech. Behav. Biomed. Mater.*, 2019, **90**, 191–201.
25 M. H. Chen, L. L. Wang, J. J. Chung, Y. H. Kim, P. Atluri and J. A. Burdick, *ACS Biomater. Sci. Eng.*, 2017, **3**, 3146–3160.
26 A. M. Sisso, M. O. Boit and C. A. DeForest, *J. Biomed. Mater. Res., Part A*, 2020, **108**, 1112–1121.
27 S. Samimi, S. Gharaie, S. Dabiri and M. Akbari, *Polymers*, 2018, **10**, 1317.
28 C. B. Highley, C. B. Rodell and J. A. Burdick, *Adv. Mater.*, 2015, **27**, 5075–5079.
29 P. T. Smith, A. Basu, A. Saha and A. Nelson, *Polymer*, 2018, **152**, 42–50.
30 J. A. Lewis, *Adv. Funct. Mater.*, 2006, **16**, 2193–2204.
31 M. Jalaal, G. Cottrell, N. Balmforth and B. Stoeber, *J. Rheol.*, 2017, **61**, 139–146.
32 D. Chimene, R. Kaunas and A. K. Gaharwar, *Adv. Mater.*, 2020, **32**, 1902026.
33 C. Loebel, A. Ayoub, J. H. Galarraga, O. Kossover, H. Simaan-Yameen, D. Seliktar and J. A. Burdick, *J. Mater. Chem. B*, 2019, **7**, 1753–1760.
34 C. R. Fellin, S. M. Adelmund, D. G. Karis, R. T. Shafranek, R. J. Ono, C. G. Martin, T. G. Johnston, C. A. DeForest and A. Nelson, *Polym. Int.*, 2019, **68**, 1238–1246.
35 R. T. Shafranek, J. D. Leger, S. Zhang, M. Khalil, X. Gu and A. Nelson, *Mol. Syst. Des. Eng.*, 2019, **4**, 91–102.
36 D. G. Karis, R. J. Ono, M. Zhang, A. Vora, D. Storti, M. A. Ganter and A. Nelson, *Polym. Chem.*, 2017, **8**, 4199–4206.
37 A. Basu, A. Saha, C. Goodman, R. T. Shafranek and A. Nelson, *ACS Appl. Mater. Interfaces*, 2017, **9**, 40898–40904.
38 S. C. Millik, A. M. Dostie, D. G. Karis, P. T. Smith, M. McKenna, N. Chan, C. D. Curtis, E. Nance, A. B. Theberge and A. Nelson, *Biofabrication*, 2019, **11**, 045009.
39 T. G. Johnston, S. F. Yuan, J. M. Wagner, X. Yi, A. Saha, P. Smith, A. Nelson and H. S. Alper, *Nat. Commun.*, 2020, **11**, 1–11.
40 J. Wong, A. T. Gong, P. A. Defnet, L. Meabe, B. Beauchamp, R. M. Sweet, H. Sardon, C. L. Cobb and A. Nelson, *Adv. Mater. Technol.*, 2019, **4**, 1900452.
41 A. Saha, T. G. Johnston, R. T. Shafranek, C. J. Goodman, J. G. Zalatan, D. W. Storti, M. A. Ganter and A. Nelson, *ACS Appl. Mater. Interfaces*, 2018, **10**, 13373–13380.
42 S. Dutta and D. Cohn, *J. Mater. Chem. B*, 2017, **5**, 9514–9521.
43 M. Müller, J. Becher, M. Schnabelrauch and M. Zenobi-Wong, *Biofabrication*, 2015, **7**, 035006.
44 B. D. Fairbanks, D. M. Love and C. N. Bowman, *Macromol. Chem. Phys.*, 2017, **218**, 1700073.
45 C. Resetco, B. Hendriks, N. Badi and F. Du Prez, *Mater. Horiz.*, 2017, **4**, 1041–1053.
46 A. B. Lowe, *Polym. Chem.*, 2014, **5**, 4820–4870.
47 R. Alonso, P. Jiménez-Meneses, J. García-Rupérez, M. J. Bañuls and Á. Maquieira, *Chem. Commun.*, 2018, **54**, 6144–6147.
48 J. C. Grim, T. E. Brown, B. A. Aguado, D. A. Chapnick, A. L. Viert, X. Liu and K. S. Anseth, *ACS Cent. Sci.*, 2018, **4**, 909–916.
49 Y. Liu, W. Hou, H. Sun, C. Cui, L. Zhang, Y. Jiang, Y. Wu, Y. Wang, J. Li, B. S. Sumerlin, Q. Liu and W. Tan, *Chem. Sci.*, 2017, **8**, 6182–6187.
50 K. L. Killops, L. M. Campos and C. J. Hawker, *J. Am. Chem. Soc.*, 2008, **130**, 5062–5064.
51 B. Colak, S. Di Cio and J. E. Gautrot, *Biomacromolecules*, 2018, **19**, 1445–1455.
52 S. Stichler, T. Jungst, M. Schamel, I. Zilkowski, M. Kuhlmann, T. Böck, T. Blunk, J. Teßmar and J. Groll, *Ann. Biomed. Eng.*, 2017, **45**, 273–285.

53 H. Shih and C. C. Lin, *Biomacromolecules*, 2012, **13**, 2003–2012.
54 L. A. Sawicki and A. M. Kloxin, *Biomater. Sci.*, 2014, **2**, 1612–1626.
55 S. Lee, H. Tae and C. S. Ki, *Carbohydr. Polym.*, 2017, **167**, 270–279.
56 L. Maleki, U. Edlund and A. C. Albertsson, *Carbohydr. Polym.*, 2017, **170**, 254–263.
57 D. P. Nair, M. Podgórski, S. Chatani, T. Gong, W. Xi, C. R. Fenoli and C. N. Bowman, *Chem. Mater.*, 2014, **26**, 724–744.
58 B. H. Northrop and R. N. Coffey, *J. Am. Chem. Soc.*, 2012, **134**, 13804–13817.
59 S. Huang, J. Sinha, M. Podgórski, X. Zhang, M. Claudino and C. N. Bowman, *Macromolecules*, 2018, **51**, 5979–5988.
60 L. Lecamp, F. Houllier, B. Youssef and C. Bunel, *Polymer*, 2001, **42**, 2727–2736.
61 J. M. Sirrine, V. Meenakshisundaram, N. G. Moon, P. J. Scott, R. J. Mondschein, T. F. Weiseman, C. B. Williams and T. E. Long, *Polymer*, 2018, **152**, 25–34.
62 D. R. Berry, B. K. Díaz, A. Durand-Silva and R. A. Smaldone, *Polym. Chem.*, 2019, **10**, 5979–5984.
63 A. E. Rydholm, C. N. Bowman and K. S. Anseth, *Biomaterials*, 2005, **26**, 4495–4506.
64 P. J. Scott, V. Meenakshisundaram, N. A. Chartrain, J. M. Sirrine, C. B. Williams and T. E. Long, *ACS Appl. Polym. Mater.*, 2019, **1**, 684–690.
65 M. Rubinstein and R. Colby, *Polymer Physics*, Oxford University Press, New York, 2003, p. 440.
66 J. Jiang, C. Burger, C. Li, J. Li, M. Y. Lin, R. H. Colby, M. H. Rafailovich and J. C. Sokolov, *Macromolecules*, 2007, **40**, 4016–4022.
67 M. Sen, A. Yakar and O. Güven, *Polymer*, 1999, **40**, 2969–2974.
68 A. C. Jimenez-Vergara, J. Lewis, M. S. Hahn and D. J. Munoz-Pinto, *J. Biomed. Mater. Res., Part B*, 2018, **106**, 1339–1348.
69 C. G. Rodriguez, M. Chwatko, J. Park, C. L. Bentley, B. D. Freeman and N. A. Lynd, *Macromolecules*, 2020, **53**, 1191–1198.